



HAL
open science

The $\nu_1 + 3\nu_3$ absorption band of nitrogen dioxide ($^{14}\text{N}^{16}\text{O}_2$) by CRDS near 6000 cm^{-1}

O.V. Naumenko, A.A. Lukashevskaya, S. Kassi, S. Béguier, A. Campargue

► **To cite this version:**

O.V. Naumenko, A.A. Lukashevskaya, S. Kassi, S. Béguier, A. Campargue. The $\nu_1 + 3\nu_3$ absorption band of nitrogen dioxide ($^{14}\text{N}^{16}\text{O}_2$) by CRDS near 6000 cm^{-1} . *Journal of Quantitative Spectroscopy and Radiative Transfer*, 2019, 232, pp.146-151. 10.1016/j.jqsrt.2019.04.029 . hal-02271441

HAL Id: hal-02271441

<https://hal.science/hal-02271441>

Submitted on 22 Oct 2021

HAL is a multi-disciplinary open access archive for the deposit and dissemination of scientific research documents, whether they are published or not. The documents may come from teaching and research institutions in France or abroad, or from public or private research centers.

L'archive ouverte pluridisciplinaire **HAL**, est destinée au dépôt et à la diffusion de documents scientifiques de niveau recherche, publiés ou non, émanant des établissements d'enseignement et de recherche français ou étrangers, des laboratoires publics ou privés.



Distributed under a Creative Commons Attribution - NonCommercial 4.0 International License

The $\nu_1+3\nu_3$ absorption band of nitrogen dioxide ($^{14}\text{N}^{16}\text{O}_2$) by CRDS near 6000 cm^{-1}

O. V. Naumenko¹, A. V. Lukashevskaya¹, S. Kassi², S. Béguier² and A. Campargue^{2*}

¹ *Laboratory of Theoretical Spectroscopy, V. E. Zuev Institute of Atmospheric Optics, Siberian Branch, Russian Academy of Sciences, 1, Academician Zuev sq., Tomsk 634055, Russia*

² *Univ. Grenoble Alpes, LIPhy, F-38000 Grenoble, France*

Key words: Nitrogen dioxide; NO_2 ; cavity ring down spectroscopy; CRDS; electron spin-rotation interaction; effective Hamiltonian

Number of pages: 15

Number of tables: 2

Number of figures: 8

* Corresponding author: Alain.Campargue@univ-grenoble-alpes.fr

Abstract

The high resolution absorption spectrum of the NO₂ molecule is recorded between 5855 and 6006 cm⁻¹ by high sensitivity cavity ring down spectroscopy (CRDS). Positions and intensities in the 5×10⁻²⁷-4×10⁻²³ cm/molecule range are derived from the profile fitting of more than 7500 lines. The absorption is dominated by the transitions of the (103)-(000) vibrational band centered at 5984.704 cm⁻¹. The spectrum is assigned and modeled using an effective Hamiltonian (EH) which explicitly takes into account a spin-rotational interaction and interaction of the (103) bright state with three “dark” states: (122), (080) and (410). The ν₁+3ν₃ band was already analyzed by Fourier transform spectroscopy in Miljanic S., Perrin A., Orphal J., Fellows C.E., Chélin, J. Mol. Spectrosc. 2008, V. 251, P. 9-15, where resonance interactions between the (103) state and the (122) and (080) “dark” states were taken into account. More than 3000 lines are presently assigned with rotational quantum numbers *N* and *K_a* up to 59 and 13, respectively, while 1147 transitions with maximum *N* and *K_a* values of 47 and 8, respectively, were previously identified by FTS. The measured line positions are reproduced with an (obs.-calc.) *rms* of 0.0023 cm⁻¹ by variation of 41 EH parameters. About 80 transitions reaching the (080) highly excited bending upper state and borrowing their intensity from the resonance coupling with the (103)-(000) band were assigned for the first time. The main parameter in the transition moment series of the ν₁+3ν₃ band is determined from the fitting of the measured intensities.

1. Introduction

The NO₂ molecule contributes to the pollution of the troposphere as well as to the ozone layer depletion. Its absorption spectrum is of interest not only for our atmosphere but also for astrophysical objects like exoplanets (see for example [1] and references quoted therein). Experimental rotation-vibration NO₂ transitions from about 20 original sources in the 0-7920 cm⁻¹ spectral range were recently involved in global fitting of the line positions [2]. The results of some experimental studies were included in the last versions of the HITRAN [3] and GEISA [4] databases. However, these databases do not contain line parameters of NO₂ above 3074 cm⁻¹. Since 2010, we have been systematically investigating the weak NO₂ spectrum in the 5800-8000 cm⁻¹ region by high-sensitivity cavity ring down spectroscopy (CRDS). A ten of new absorption bands were assigned and modeled in the frame of the effective Hamiltonian (EH) model [5-12].

This work is devoted to the analysis of the CRDS NO₂ spectrum in the 5855-6006 cm⁻¹ region. The vibrational-rotation transitions of the $\nu_1+3\nu_3$ band at 5984.7 cm⁻¹ dominate the spectrum. This band is the strongest vibrational band above 5800 cm⁻¹. Its first study was reported in 1970 by Blank et al. [13]. More recently, it was analyzed from a spectrum of a NO₂/NO/ICl mixture recorded by Fourier transform spectroscopy [14]. 1147 transitions with N up to 47 and K_a up to 8 were identified and modeled. Only a very approximate value of the band intensity was reported in Ref. [14] based on an estimated value of the NO₂ partial pressure in the used gas mixture. In the present work, we report an extended analysis of 3154 identified ¹⁴N¹⁶O₂ transitions with accurately measured positions and intensities up to N and K_a rotational quantum numbers of 59 and 13, respectively.

2. Experimental details and line parameters retrieval

The reader is referred to Refs. [15,16] for a detailed description of the used fiber-connected cavity ring down spectrometer. Seven Distributed Feedback (DFB) laser diodes were used as light sources to cover the 5855–6006 cm⁻¹ spectral region under study. The frequency calibration was performed using a commercial Fizeau type wavemeter. We estimate the accuracy on the line position to be 1×10^{-3} cm⁻¹ for well isolated lines. The considered NO₂ band is not very weak which makes possible to use low pressure for the recordings. Most of the forthcoming data analysis relies on a spectrum recorded at a pressure of 0.05 Torr measured by a capacitance gauge (MKS, Baratron 626B 1.0 Torr, 0.15% accuracy of the reading), only, and a temperature of 297.3 K. Additional recordings at 1.0 Torr were used for the lower energy region below 5910 cm⁻¹. **Fig. 1** shows an overview of the 0.05 Torr recordings. The successive

zooms included in this figure illustrate the sensitivity of the recordings and the high dynamic on the intensity scale. The noise-equivalent absorption of the spectrum is on the order of $\alpha_{min} \sim 1 \times 10^{-10} \text{ cm}^{-1}$. For these low pressure values, the dimerization is very limited and N_2O_4 concentration can be neglected.

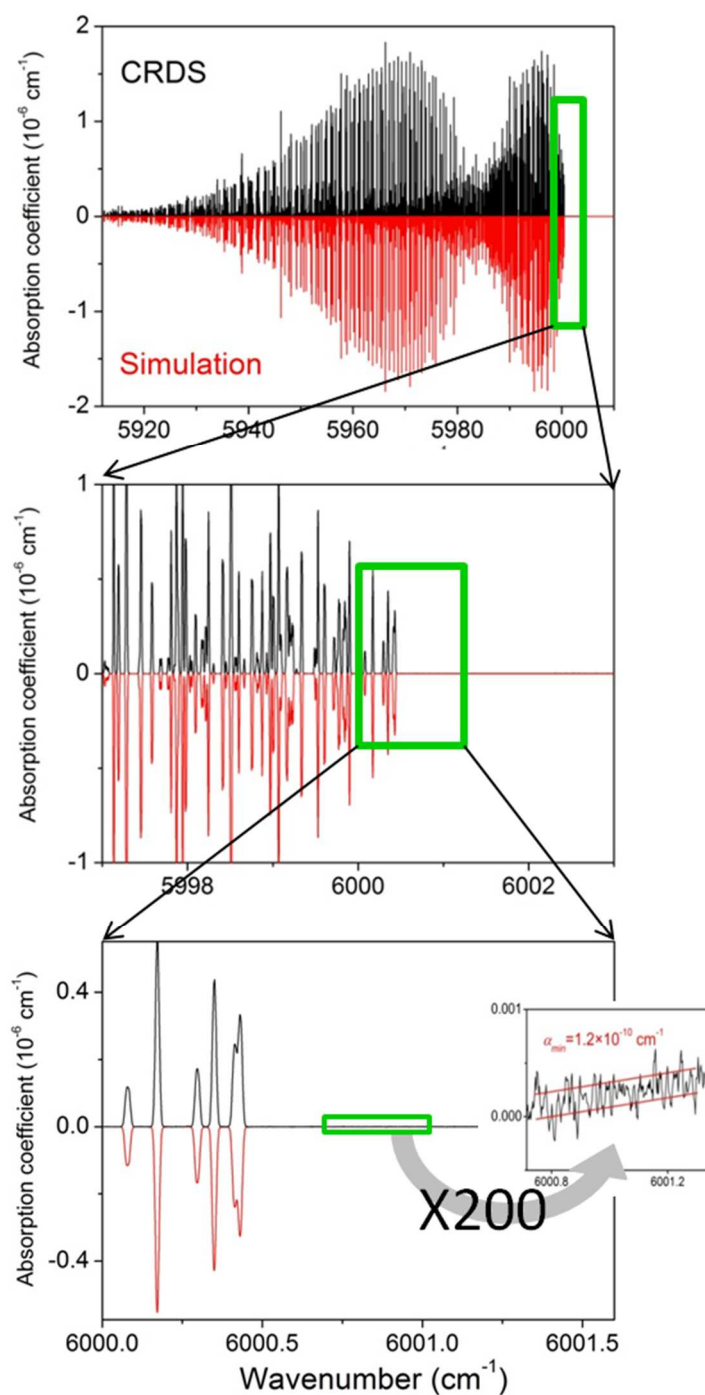


Fig. 1. Comparison of the CRDS spectrum of the v_1+3v_3 band of NO_2 recorded at 0.05 Torr to a simulation using the effective operator approach.

The line parameter retrieval was performed using an homemade multiline fitting

program. The spectral line shape used at 0.05 Torr is very close to a Doppler profile. Nevertheless, the achieved signal to noise ratio of the spectrum requires using a Voigt profile for some strong lines. Note that in the case of unresolved spin-rotational doublets, we often fitted the absorption feature as a single line. The line list retrieved from the 0.05 Torr spectra includes 3420 lines in the 5911-6005 cm^{-1} region with intensities ranging between 10^{-26} and 10^{-23} $\text{cm}/\text{molecule}$ at 297 K. A separate list of about 3500 lines was constructed from the 1 Torr recordings in the 5854-5911 cm^{-1} region. Only a small fraction of this set of weak lines (intensities in the 10^{-27} - 10^{-25} $\text{cm}/\text{molecule}$ range) belongs to the $\nu_1+3\nu_3$ band.

3. Spectrum assignment and line position modeling

The overview of the experimental spectrum is displayed on the upper panel of **Fig. 1**. The spectrum was assigned on the basis of EH calculations which account for explicitly the spin-rotational interactions as well as rotation-vibration resonance coupling. The resonance scheme proposed in Ref. [14] is confirmed by the present analysis. It involves a strong interaction of the (103) bright state with two dark states - (122) and (080) - already included in Ref. [14] and a newly evidenced interaction with the (410) nearby dark state. The scheme of the effective Hamiltonian matrix is presented in **Fig. 2**.

	(103)	(122)	(410)	(080)
(103)	$H_{VR}+H_{SR}$	H^C	H^C	H^C
(122)	H^C	$H_{VR}+H_{SR}$		
(410)	H^C		$H_{VR}+H_{SR}$	
(080)	H^C			$H_{VR}+H_{SR}$

Scheme of $H_{VR}+H_{SR}$, V-diagonal block:

		(V_1, V_2, V_3)	
		$N=J-1/2$	$N=J+1/2$
(V_1, V_2, V_3)	$N=J-1/2$	$H_{VR}+H_{SR}$	H_{SR}
	$N=J+1/2$	H_{SR}	$H_{VR}+H_{SR}$

Scheme of H^C , V-off diagonal block:

		(V_1, V_2, V_3)	
		$N=J-1/2$	$N=J+1/2$
(V'_1, V'_2, V'_3)	$N=J-1/2$	H^C	
	$N=J+1/2$		H^C

Fig.2. Scheme of the H^{eff} matrix.

The reader is referred to Ref. [17] for the explicit expression of the Watson-type Hamiltonian (H_{VR}), and to Ref. [18] for the electron spin-rotation interaction operator (H_{SR}).

Note that the V -off diagonal block does not include an anharmonic interaction term. The Coriolis interaction operator was used in the following form:

$$H^C = C_0 iN_Y + C_K \{N_X, N_Z\} + C_{KK} \{iN_Y, N_Z^2\} + C_{KKK} \{\{N_X, N_Z\}, N_Z^2\} + C_{NK} \{N_X, N_Z\} N^2 + C_{KKN} \{iN_Y, N_Z^2\} N^2 \quad (1)$$

$C_0, C_K, C_{KK}, C_{KKK}, C_{NK}, C_{KKN}$, are the Coriolis coupling constants and the parameters describing their rotational dependence.

The values of the spectroscopic parameters derived in Ref. [14] were used as initial parameters. As soon as new rotation-vibration transitions were assigned, the spectroscopic parameters were refined from the fitting to observed positions and intensities providing more accurate spectrum simulation for further identification. Resonance interactions are discussed in details below. For poorly resolved SR doublets or strongly blended lines, the calculated line positions might be more accurate than experimental values. The summary of the assignments obtained from the spectrum analysis is presented in **Table 1**. A final *rms* deviation of 0.0023 cm^{-1} was achieved by varying 41 parameters listed in **Table 2**.

Table 1 includes a comparison to the results reported in Ref. [14]. About 3 times more transitions were assigned (3154 vs 1147) with maximal N and K_a rotational quantum numbers equal to 59 and 13, respectively, while only transitions with $N \leq 47$ and $K_a \leq 8$ were identified in Ref. [14]. Overall, the average and *rms* deviation of the differences of the FTS and CRDS position values are 0.0016 and 0.0020 cm^{-1} , respectively for 1038 transitions (corresponding to 92 % of the transitions measured by FTS). We note a significant decrease of the *rms* deviation if only well resolved or fully degenerate lines are considered. On the opposite, comparison of our measured doublet positions with those calculated using the parameters of Ref. [14] resulted in an *rms* deviation of 0.0028 cm^{-1} for 692 lines while a value of 0.0010 cm^{-1} is obtained using our parameters, confirming that our peaklist provides better accuracy for close lying spectral lines.

Taking into account multiple assignments attached to the same observed line, 2754 NO_2 absorption lines were identified in the large set of about 7500 measured lines. The assigned lines bring 94% of the total selective absorption in the considered spectral region. The large set of weak unidentified lines may belong to the (103)-(000) band of minor NO_2 isotopologues, to "hot" bands of the main isotopologue originating from the (010) lower vibrational state or to impurities.

Table 1. Summary of the assignments

State	Vib. term, cm ⁻¹	Number of lines	N_{max}	K_{amax}
(103)	5984.704	2878(1087 ^b)	59(47 ^b)	13(8 ^b)
(122)	5898.94 ^a	192(60 ^b)	45(34 ^b)	5
(080)	5965.61 ^a	81	47	4
(410)	5930.66 ^a	3	50	3

Notes:^a Vibrational term value obtained by LIDFS [19]^b Value from Ref. [14]

Table 2.Spectroscopic parameters for the {(103),(122),(410),(080)} interacting vibrational states of NO₂ in cm⁻¹

Parameter	(000) ^a	(103)	(122)	(410)	(080)
E_v	0	5984.7041266(1721) 5984.705 ^b	5898.94 ^b	5930.66 ^b	5965.61 ^b
A	8.00235469	7.41131179(2600)	8.3329234(4700)	8.653730(7800)	12.5472741(1700)
$(B+C)/2$	0.422074669	0.4112220702(7200)	0.412461271(3600)	0.41248350(2700)	0.40723230(3100)
$(B-C)/4(10^{-2})$	0.58160645	0.60155475(4300)	0.620654(1600)	0.564 ^c	0.8308 ^c
$\Delta_K(10^{-2})$	0.26878757	0.2392589(1100)	0.220699(1900)		1.18 ^c
$\Delta_{NK}(10^{-4})$	-0.196822	-0.2986780(9900)	-0.484637(1600)	-0.219 ^c	-3.66307(1900)
$\Delta_N(10^{-6})$	0.2992447	0.3160513(1000)		0.311 ^c	0.302 ^c
$\delta_K(10^{-5})$	0.40547	0.691033(4500)			42.89315(7000)
$\delta_N(10^{-7})$	0.3192774	0.3621363(9100)		0.332 ^c	0.153 ^c
$H_K(10^{-5})$	0.3031569	0.285941(1200)			3.030 ^c
$H_{KN}(10^{-7})$	-0.27044			-0.262 ^c	-0.261 ^c
$H_{NK}(10^{-10})$	0.2995			0.152 ^c	0.151 ^c
$H_M(10^{-12})$	0.2866				1.126 ^c
$h_K(10^{-7})$	0.29297				
$h_{KN}(10^{-10})$	-0.3637				
$h_M(10^{-12})$	0.1057			0.246 ^c	0.246 ^c
$L_K(10^{-8})$	-0.51104	-0.58591(1200)		1.43 ^c	-6.90 ^c
$L_{KN}(10^{-10})$	0.35117	-1.79264(7300)		0.301 ^c	0.301 ^c
$L_{KN}(10^{-12})$	0.12158			0.138 ^c	0.138 ^c
$P_K(10^{-11})$	0.867	1.12975(2900)			
$Q_K(10^{-14})$	-0.8439				
Spin-rotational parameters					
ϵ_{aa}	0.180353	0.15764945(9200)	0.1988798(3000)		0.77205(8100)
$(\epsilon_{bb}+\epsilon_{cc})/2(10^{-2})$	-0.1460137	-0.1611325(4400)	-0.173315(1800)	-0.1619 ^c	0.15282(1700)
$(\epsilon_{bb}-\epsilon_{cc})/4(10^{-3})$	0.858985	0.943954(6200)		0.853 ^c	-11.1645(9400)
$\delta_{KS}(10^{-6})$	0.3769				
$\delta_{NS}(10^{-7})$	0.244				
$\Delta_{KS}(10^{-3})$	-0.17606	-0.1594140(7700)		-0.241 ^c	-0.697 ^c
$\Delta_{NS}(10^{-9})$	0.6322				
$\Delta_{NKS}(10^{-5})$	0.1678	0.280935(1200)			
$\Delta_{KNS}(10^{-5})$	-0.10775			0	
$H_{KS}(10^{-6})$	0.29673			0.3096 ^c	0.309 ^c
$L_{KS}(10^{-9})$	-0.35689			-0.398 ^c	-0.398 ^c

Coriolis resonances

Parameter	(103) \leftrightarrow (122)	(103) \leftrightarrow (080)	(103) \leftrightarrow (410)
$C^2_o(10^{-1})$	-0.4561674(3200)		0.0602384(2000)
$C^2_{KK}(10^{-3})$	0.922150(5600)		
$C^2_{KKK}(10^{-3})$	-0.095351(9900)		
$C^2_{NK}(10^{-6})$	-0.187088(2100)	-0.436370(4700)	
$C^2_{KKN}(10^{-7})$		-0.25899(1300)	

Notes

1 σ confidential intervals are given in unit of the last digit. In absence of parameter value, the parameter was constrained to the ground state value of Ref. [20] given in the 2nd column

^a Ref. [20]

^b Ref. [19]

^c Ref. [2]

4. Spin-rotation splittings

The SR splittings due to the $S=1/2$ electronic spin of the \tilde{X}^2A_1 ground electronic state are a characteristic feature of the NO₂ rovibrational spectrum. The SR splittings can provide an additional criterion for the assignments. Due to the low pressure of the recordings, line profiles are mostly Doppler limited (HWHM of 0.0054 cm⁻¹) and SR doublets with splitting as low as

0.003 cm⁻¹ could be resolved, though the accuracy of experimental positions in this case may be lower than that for isolated line. In general, SR splittings smoothly depend on N and K_a rotational quantum numbers increasing with K_a and decreasing with N for a given K_a value. This is indeed what it is observed for the (103) state as illustrated on **Fig. 3**.

The resonance interaction between the (103) and (080) dark state destroys the smooth dependence of their SR splittings on the N rotational quantum number, as illustrated in **Fig. 4**. Note that, within the resonance range ($24 < N < 40$), the measured and calculated SR splittings of the $K_a=5$ (103) and $K_a=4$ (080) interacting energy levels deviate importantly from those of Ref. [14]. We cannot rule out that this perturbed behavior combined with a limited set of observations resulted in distortion of some of the (080) varied SR parameters.

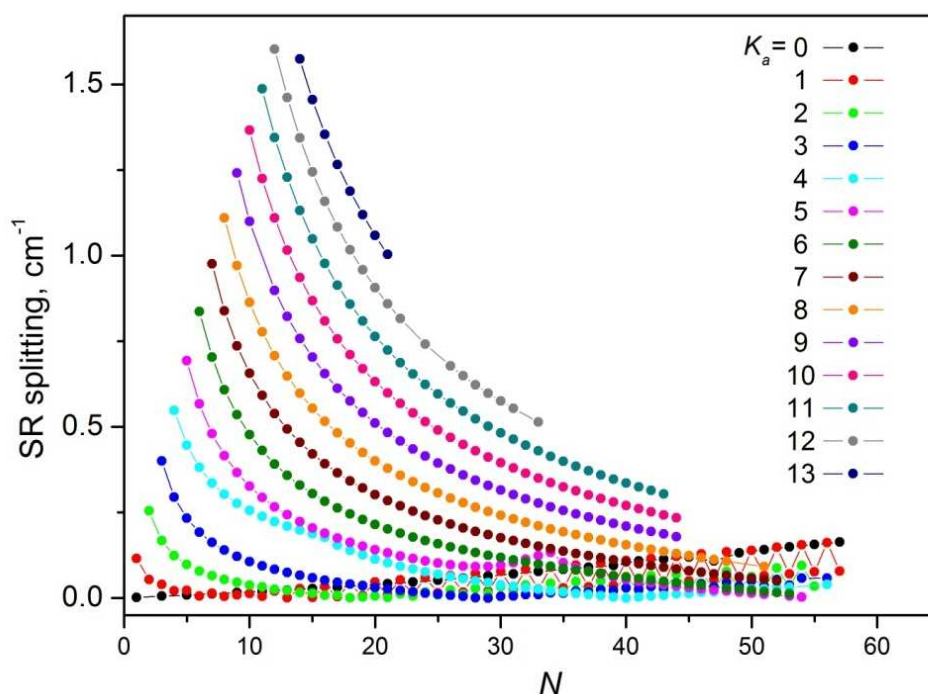


Fig. 3. Calculated spin–rotation splitting of the energy levels of the (103) vibrational state. The plot is limited to the observed levels.

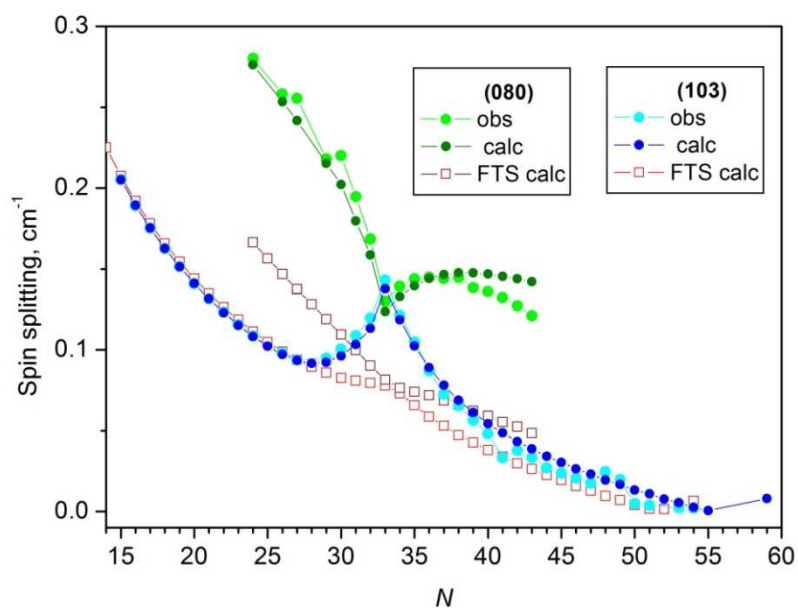


Fig. 4. SR splittings of the $K_a=5$ (103) and $K_a=4$ (080) energy levels involved in resonance interaction. The FTS calculated values [14] are compared to our measured and calculated values.

5. Resonance interactions and intensity transfer

The strong couplings of the (122) and (080) dark states with the (103) bright state have a local character and affect only definite K_a series. The (103)-(122) interaction links $K_a=4$ (103) and $K_a=5$ (122) energy levels, while the (103)-(080) resonance couples $K_a=5$ (103) and $K_a=4$ (080) levels. The rotational dependence of the resonance mixing coefficients of the resulting rotation-vibration wavefunctions of the (103) state is illustrated on **Fig. 5**.

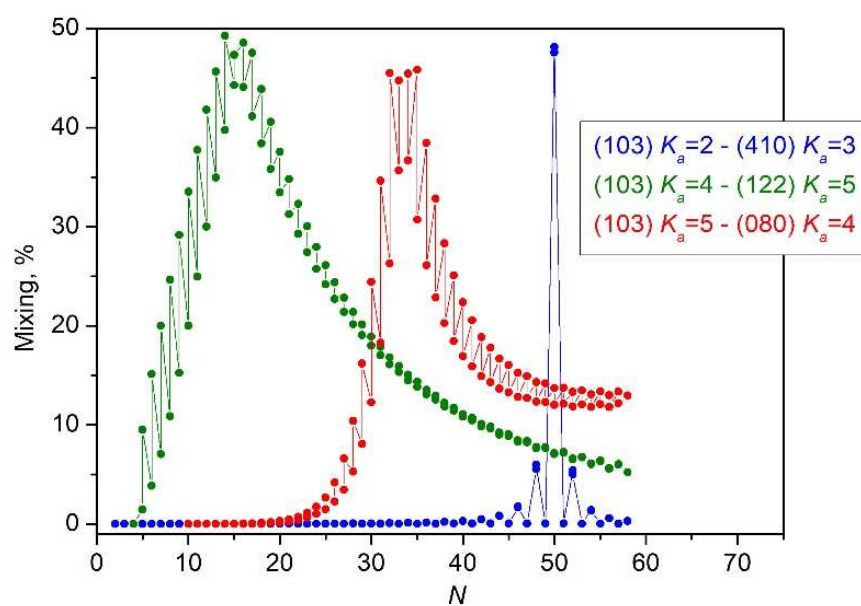


Fig. 5. Mixing coefficients for the (103) wavefunctions due to resonance interaction with the (122), (080) and (410) vibrational states.

The (103)-(122) resonance interaction starts at $N=5$ and reaches a maximum at $N=15$ (50% mixing of the wavefunctions). The resonance mixing induces intensity transfers from the (103)-(000) transitions to their (122)-(000) counterparts which become observable, as illustrated in **Fig. 6**. 192 transitions of the (122)-(000) band were assigned (compared to 60 in Ref. [14]).

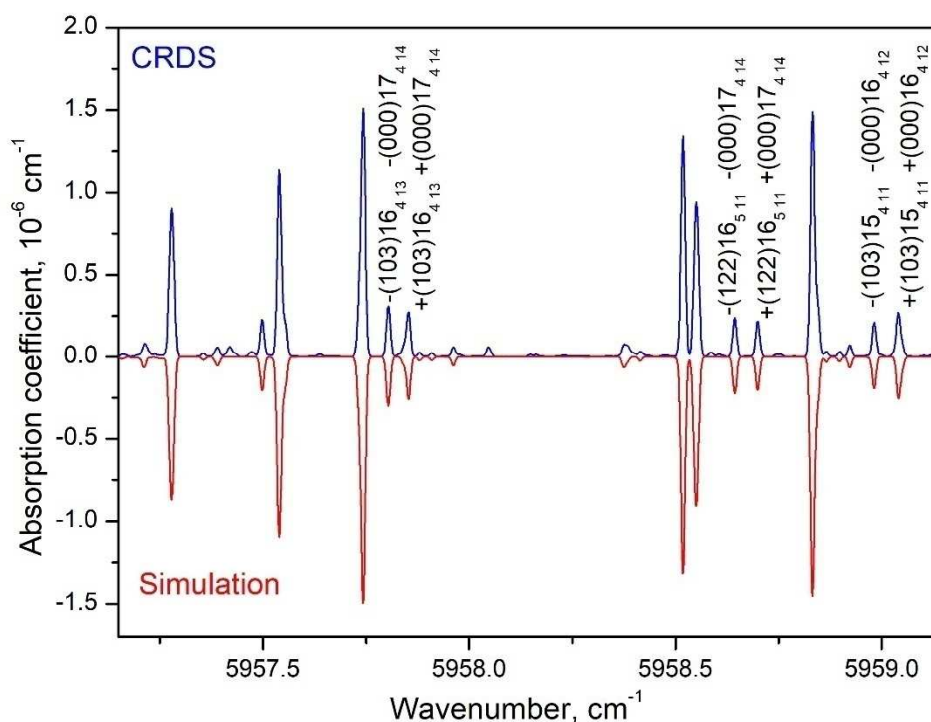


Fig. 6.

Part of the CRDS NO_2 spectrum around 5958 cm^{-1} . Lines of the (122)-(000) and (103)-(000) bands coming on the upper levels in close resonance are indicated.

Upper panel: CRDS spectrum ($P=0.05$ Torr)

Lower panel: Simulated spectrum

The strong (103)-(080) resonance induces a maximal mixing of about 48% for $N=35$. 81 transitions belonging to the highly excited $8\nu_2$ bending band were assigned for the first time (**Fig. 7**). The corresponding line positions could be reproduced by varying both some diagonal (080) state parameters and the (103)-(080) coupling constants (see **Table 2**). However, it turned out that some (080) parameters responsible for SR splittings seem to be distorted compared to those derived in Ref. [14]. In fact, all the fitted parameters of the (080) state should be considered as effective parameters allowing to reproduce satisfactorily the (080)-(000) $K_a=4$ line positions for J values between 23 and 43 (see also next Section).

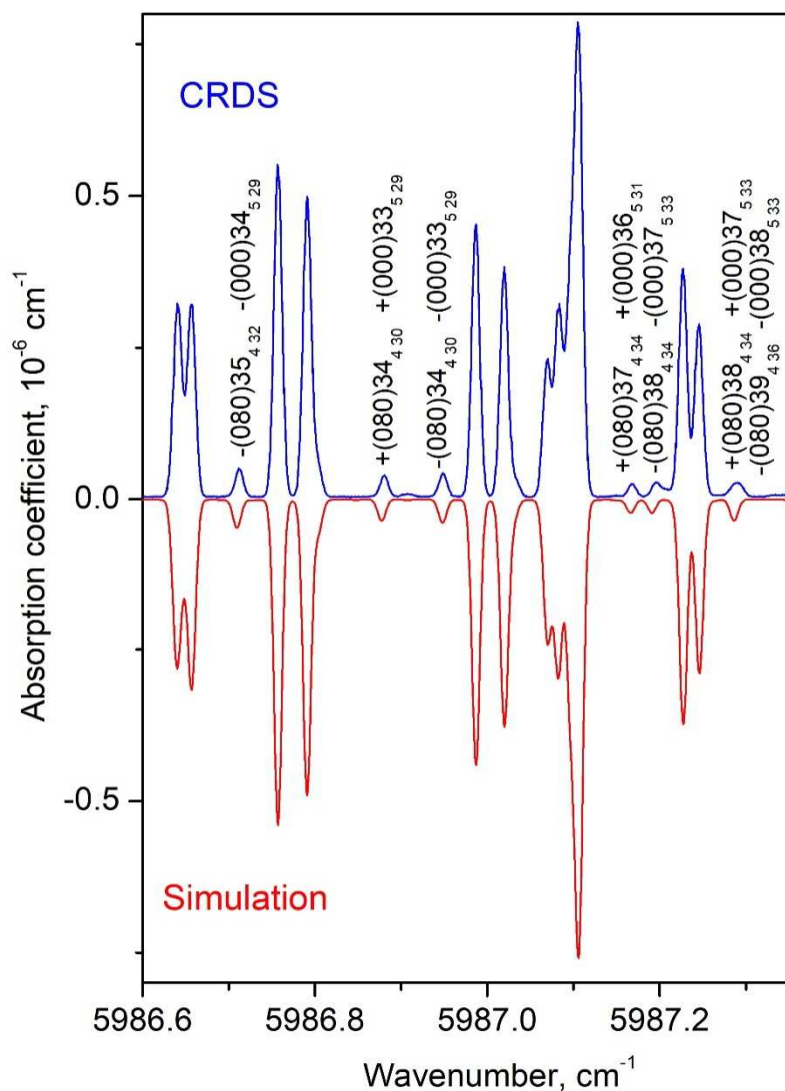


Fig. 7.

Part of the CRDS NO_2 spectrum near 5986 cm^{-1} . Weak lines assigned to the $8\nu_2$ band are indicated.

At the final stage of the spectrum assignment, the calculated positions of the $K_a=2$ series of the (103)-(000) band were found to deviate importantly (up to 0.25 cm^{-1}) from their measured values for N between 44 and 54. These line position perturbations were interpreted as due to an additional resonance interaction between (103) and the (410) vibrational dark state at 5930.66 cm^{-1} [19]. Although affecting a limited range of N values, the (103)-(410) resonance results in a strong (48%) resonance mixing for the (103) 50 2 49 SR energy levels and is confirmed by the observation of 3 transitions reaching the 50 3 47 SR upper levels of the (410) state.

6. Line intensity modeling

The absorption line intensity, $S_{b \leftarrow a}(T)$ of a $b \leftarrow a$ vibration-rotation transition (in $\text{cm}^2/\text{molecule}$), is given by:

$$S_{b \leftarrow a}(T) = \frac{8\pi^3}{3hc} C v_{b \leftarrow a} \frac{\exp(-hcE_a/kT)}{Q(T)} [1 - \exp(-hcv_{b \leftarrow a})/kT] W_{b \leftarrow a}, \quad (3)$$

where T is the temperature in K , C is the isotopic abundance ($C=0.991616$ for the main $^{14}\text{N}^{16}\text{O}_2$ isotopologue), $v_{b \leftarrow a}$ is the wavenumber of the vibration-rotation-spin transition $b \leftarrow a$, E_a is the energy of the lower state, c is the velocity of light, h is the Plank constant, k is the Boltzmann constant, $Q(T)$ is the partition function and $W_{b \leftarrow a}$ is the transition dipole moment squared. The partition function $Q(297\text{ K})=1.365162 \times 10^4$ was taken from Ref. [21]. The equation for the transition dipole moment squared of the $V'N'K'_aK'_cJ' \leftarrow VNK_aK_cJ$ transition derived in Ref. [22] in our case can be written in the following form:

$$W_{V'N'K'_aK'_cJ' \leftarrow V=0\ NK_aK_cJ} = \left| \sum_{N_0N'_0} \sum_{K\Delta K} C_{V'N'K'_aK'_cJ'}^{1\ 0\ 3\ N'_0\ K+\Delta K} C_{V=0\ NK_aK_cJ}^{0\ 0\ 0\ N_0K} G(J, J', N_0, N'_0) M_{103} \Phi_{\Delta N_0, 0}(N_0, K) \right|^2 \quad (4)$$

Here $C_{V'N'K'_aK'_cJ'}^{1\ 0\ 3\ N'_0\ K+\Delta K}$ and $C_{V=0\ NK_aK_cJ}^{0\ 0\ 0\ N_0K}$ are the expansion coefficients determining the eigenfunction of the effective Hamiltonian for the upper and lower vibration-spin-rotation states respectively, $G(J, J', N_0, N'_0)$ are the functions describing the intensity redistribution between transitions with different spin components, M_{103} is the effective dipole moment parameter, $\Phi_{\Delta N_0, 0}(N_0, K)$ is equal to the $(10JK|J'K)$ Clebsh-Gordan coefficient. The explicit equation for $G(J, J', N_0, N'_0)$ is given in Ref. [22].

The main parameter in the transition moment series ($M_I=1.12592(80) \times 10^{-3}$ Debye), was sufficient to reproduce the selected set of 713 experimental intensities with an *rms* deviation of 3.7%. The very small quoted error bar corresponds to the statistical error of the fit, the real error bar being considerably larger, probably on the order of 10 %). The agreement of the CRDS and simulated spectra is illustrated on **Figs. 1, 6** and **7**. It is worth underlining that the intensity of the weak lines of the dark bands resulting from an intensity transfer from the (103)-(000) band are very well reproduced (see **Figs. 6** and **7**) while all transition moment parameters of the (122) and (080) dark states were fixed to zero.

In case of a line corresponding to an overlapped SR doublet, as a rule, the intensity value provided by the line profile fitting is more accurate for the sum of the SR doublet than for each of the individual component. Indeed, the line intensity modeling showed a number of large (Meas.-Calc.) deviations for the SR components while the sum of measured and calculated intensities of the blended line agree very well. In these cases of close SR doublets (separation $< 0.005\text{ cm}^{-1}$), the calculated intensities may be more accurate than the measured values.

In the FTS study of Ref. [14], the band was analysed from a spectrum of a $\text{NO}_2/\text{NO}/\text{ICI}$ mixture where the sum of the NO_2 and NO partial pressures was less than 20 %. The band intensity reported in Ref. [14], $S = (9 \pm 4) \times 10^{-21}\text{ cm/molecule}$, is about three times larger than

measured in this work ($S= 2.96 \times 10^{-21}$ cm/molecule). We do not have a firm explanation of this strong disagreement. We checked that the intensity values derived from our recordings at 0.05 and 1 Torr are consistent within 10 % and are inclined to believe that the NO₂ partial pressure might have been strongly underestimated in the gas mixture used in Ref. [14] (no details on the determination are given in Ref. [14] and the value is not provided). New recordings with a new tank of NO₂ are suitable for a final checking and for ruling out the possible contamination (by air) or the possible degradation of NO₂ in the gas tank used for the CRDS recordings.

The list of assigned transitions of the (103)-(000), (122)-(000), (080)-(000) bands as well as 3 extra lines due to the (410)-(000) band is provided as Supplementary Material 1. The list includes measured line positions and their corresponding deviations from the calculated values, measured and calculated intensities followed by vibrational and rotational quantum numbers. Note that three "dark" bands involved in the analysis are responsible for only 4% of the total measured intensity of the assigned lines. The sum of the measured line intensities for the (122)-(000), (080)-(000), and (410)-(000) bands is 1.03×10^{-22} , 1.30×10^{-23} and 2.95×10^{-25} cm/molecule, respectively, compared to total value of 2.96×10^{-21} cm/molecule. The list of the selected experimental lines included into the intensity modeling is also provided in Supplementary Material 2.

7. Conclusion

The absorption spectrum of the NO₂ molecule between 5860 and 6000 cm⁻¹ has been revisited by high sensitivity CRDS. More than 3000 rotational-vibrational transitions were attributed to the (103)-(000), (122)-(000), (080)-(000) vibrational bands, while only 1147 transitions were previously assigned [14]. About 80 transitions belonging to the highly excited $8\nu_2$ bending band and borrowing their intensities from the resonance coupling with the strong $\nu_1+3\nu_3$ band were observed for the first time. The most significant differences compared to the FTS results of Ref. [14] concern the line (and band) intensities which are presently measured to be three times smaller than reported. SR splittings of the (103) and (080) interacting energy levels deviate by up to 0.06 cm⁻¹ from those of Ref. [14]. The observed line positions and intensities were modeled with an accuracy of 0.0023 cm⁻¹ and 3.7%, respectively, close to the experimental uncertainty, and detailed synthetic spectrum is generated limited to the observed upper energy levels. An additional resonance coupling between the (103) and (410) vibrational states was found to perturb $K_a= 2$ series of the (103) energy levels with N quantum number between 44 and 54.

Acknowledgements

This research is supported by CNRS (France) in the framework of the Laboratoire International Associé SAMIA (Spectroscopie d’Absorption des Molécules d’Intérêt Atmosphérique). This work was performed in the frame of the LabexOSUG@2020 (ANR10 LABX56). Part of the work related to the modeling of the spectrum was performed under the financial support of the Russian Science Foundation (No. 18-35-00575). We thank Prof. Perevalov V. I. (IAO SB RAS) for careful reading and discussing the manuscript.

References

1. Tennyson J, Yurchenko SN Laboratory spectra of hot molecules: Data needs for hot super - Earth exoplanets. *Mol Astrophys* 2017;8;1-18.
2. Lukashetskaya AA, Lyulin OM, Perrin A, Perevalov VI. Global modelling of NO₂ line positions. *Atmospheric and Oceanic Optics* 2015;28:216–31.
3. Rothman LS, Gordon IE, Babikov Y, Barbe A, Benner DC, Bernath PF, et al. The HITRAN2012 molecular spectroscopic database. *J Quant Spectrosc Radiat Transf* 2013;130:4–50.
4. Jacquinet-Husson N, Armante R, Crépeau N, Chédin A, Scott NA, Boutammine C, et al. The 2015 edition of the GEISA spectroscopic database. *J Mol Spectrosc* 2016;327:31–72.
5. Perrin A, Kassi S, Campargue A. First high resolution analysis of the 4v₁+v₃ band of nitrogen dioxide near 1.5 μm. *J Quant Spectrosc Radiat Transf* 2010;111:2246-55.
6. Mondelain D, Perrin A, Kassi S, Campargue A. First high resolution analysis of the 5v₃ band of nitrogen dioxide near 1.3 μm. *J Quant Spectrosc Radiat Transf* 2012; 113:1058-65.
7. Lukashetskaya AA, Naumenko OV, Perrin A, Mondelain D, Kassi S, Campargue A. High sensitivity cavity ring down spectroscopy of NO₂ between 7760 and 7917 cm⁻¹. *J Quant Spectrosc Radiat Transf* 2013;130:249–259.
8. Lukashetskaya AA, Naumenko OV, Mondelain D, Kassi S, Campargue A. High sensitivity cavity ring down spectroscopy of the 3v₁+3v₂+v₃ band of NO₂ near 7587 cm⁻¹. *J Quant Spectrosc Radiat Transf* 2016;177:225–233
9. Lukashetskaya AA, Naumenko OV, Kassi S, Campargue A. First detection and analysis of the 3v₁+v₂+v₃ band of NO₂ by CRDS near 6156 cm⁻¹. *J Quant Spectrosc Radiat Transf* 2017;338:91-96.
10. Lukashetskaya AA, Kassi S, Campargue A, Perevalov VI. High sensitivity Cavity Ring Down Spectroscopy of the 2v₁+3v₂+v₃ band of NO₂ near 1.57 μm. *J Quant Spectrosc Radiat Transf* 2017;200:17-24.
11. Lukashetskaya AA, Kassi S, Campargue A, Perevalov VI. High sensitivity Cavity Ring Down Spectroscopy of the 4v₃ band of NO₂ near 1.59 μm. *J Quant Spectrosc Radiat Transf* 2017;202:302-307.
12. Lukashetskaya AA, Mondelain D, Campargue A, Perevalov VI. High sensitivity cavity ring down spectroscopy of the v₁+4v₃ band of NO₂ near 1.34 μm. *J Quant Spectrosc Radiat Transf* 2018;219:393-398.
13. Blank RE, Olman MD, Hause CD. Upper State Molecular Constants for the (0,0,3) and (1, 0,3) Vibration-Rotation Bands of Nitrogen Dioxide. *J Mol Spectrosc*. 1970; 33,109-118.
14. Miljanic S, Perrin A, Orphal J, Fellows CE, Chelin P. New high resolution analysis of the v₁+3v₃ band of nitrogen dioxide. *J Mol Spectrosc* 2008;251:9-15.
15. Kassi S, Campargue A. Cavity ring down spectroscopy with 5×10⁻¹³ cm⁻¹ sensitivity. *J Chem Phys* 2012;137:234201.
16. Mikhailenko SN, Le Wang, Kassi S, Campargue A. Weak water absorption lines around 1.455 and 1.66 μm by CW-CRDS. *J Mol Spectrosc* 2007;244:170–8
17. Watson JKJ. Aspects of quartic and sextic centrifugal effects on rotational energy levels. In: Durig JR, editor. *Vibrational spectra and structure*; 1977. p. 1–89. New York.
18. Brown JM, Sears TJ. A reduced form of the spin-rotation Hamiltonian for asymmetric-top molecules, with applications to HO₂ and NH₂. *J Mol Spectrosc* 1979;75:111–33.
19. Delon A, Jost R. Laser induced dispersed fluorescence spectra of jet cooled NO₂: the complete set of vibrational levels up to 10,000 cm⁻¹ and the onset of the \tilde{A}^2B_2 - \tilde{X}^2A_1 vibronic interaction. *J Chem Phys* 1991;95:5686-5700.
20. Semmoud-Monnanteuil N, Colmont JM, Perrin A, Flaud JM, Camy-Peyret C. New measurements in the millimeter wave spectrum of NO₂. *J Mol Spectrosc* 1989;134:176–82.
21. Fischer J, Gamache RR, Goldman A, Rothman LS, Perrin A. Total internal partition sums for molecular species in the 2000 edition of the HITRAN database. *J Quant Spectrosc Radiat Transfer* 2003;82:401–12.
22. Malathy Devi V, Das PP, Bano A, Narahari Rao K, Flaud JM, Camy-Peyret C, et al. Diode laser measurements of intensities, N₂-broadening, and self-broadening coefficients of lines of the v₂ band of ¹⁴N¹⁶O₂. *J Mol Spectrosc* 1981;88:251–8.

CRDS of NO_2

